Available online at www.sciencedirect.com
ScienceDirect
Journal of Luminescence 127 (2007) 616–622
JOURNAL OF LUMINESCENCE
www.elsevier.com/locate/jlumin

Optical investigation of $Y_2O_3:Sm^{3+}$ nanophosphor prepared by combustion and Pechini methods

C.A. Kodaira[a], R. Stefani[b], A.S. Maia[b], M.C.F.C. Felinto[a,*], H.F. Brito[b]

[a]*Instituto de Pesquisas Energéticas e Nucleares, Av. Prof. Lineu Prestes 2242, CEP 05508-000, Cidade Universitária, São Paulo-SP, Brazil*
[b]*Instituto de Química, Universidade de São Paulo, C.P. 26077, CEP 05513-970, São Paulo-SP, Brazil*

Received 4 December 2006; received in revised form 16 March 2007; accepted 28 March 2007
Available online 7 April 2007

Abstract

Nanoparticles of trivalent samarium ion doped into yttrium oxide with attractive photoluminescent properties were prepared using combustion and Pechini methods treated at low heating temperatures. Combustion technique focused on an exothermic reaction between metal nitrates and glycine as fuel leading to the desired product where $Y_2O_3:Sm^{3+}$ nanophosphor was heated at 400, 500 and 600 °C. For Pechini method, which is based upon *in situ* polyesterification between citric acid and ethylene glycol, the phosphor material was treated only at 600 °C. The powders were characterized by X-ray diffraction, infrared absorption spectroscopy and scanning electronic microscopy. Photoluminescent study of $Y_2O_3:Sm^{3+}$ system showed the characteristic emission narrow lines containing $(J+1/2)$-manifolds of intraconfigurational $^4G_{5/2} \rightarrow {}^6H_J$ transitions ($J = \frac{5}{2}, \frac{7}{2}, \frac{9}{2}$ and $\frac{11}{2}$) of Sm^{3+} ion with the $^4G_{5/2} \rightarrow {}^6H_{7/2}$ transition ($\lambda = 609$ nm) as a prominent intensity, when excitation was monitored at 406 nm ($^6H_{5/2} \rightarrow {}^4K_{11/2}$). The luminescence decay curves suggest a mono-exponential behavior.

Keywords: Nanoparticles; Luminescence; Trivalent samarium; Yttrium oxide; Pechini and combustion methods

1. Introduction

During the past decade many efforts have been devoted to the design of luminescent nanoparticles for replacing the organic dyes commonly used in biological material labeling. The need for ultrasensitive biomolecular detection and multilabeling led to the development of original markers permitting to overcome the limitations of organic dyes [1]. Signal amplification and photostability enhancement are essential for improvement of efficient biological probes.

Nanoparticles have been used extensively in bioaffinity sensors for nucleic acids and proteins [2,3]. Nanosized materials may provide a high reactivity and beneficial physical properties such as electrical, electrochemical, optical, and magnetic, which are chemically adaptable. Therefore, Y_2O_3 doped with rare earth ions can be used as biomarker.

Y_2O_3 shows polymorphic forms, denoted as A, B and C classified as being hexagonal, monoclinic and cubic, respectively [4]. Yttrium oxide has a coordination number equal to six and forms a cubic bixbyite structure, which contains two non-equivalent yttrium S_6 and C_2 symmetry sites [5]. Owing to its centrosymmetric character in S_6 symmetry, essentially only magnetic dipole transitions can be recorded both in absorption and emission for rare earth ions [6]. However, for the non-centrosymmetric character, such as C_2 group, the f–f transitions became partially allowed by forced electric dipole due to odd parity terms in the crystal field Hamiltonian.

Generally, phosphor materials have been produced by solid state reactions [7,8]. The disadvantage of this kind of reaction is the difficulty to obtain a homogeneous product and to control particle size. Besides, this method is cumbersome due to the utilization of high temperatures (~1500 °C) with sequential grinding and firing steps. Nevertheless, combustion process is attractive owing to direct crystallization of small-sized particles, low process temperature and reduced time consumption [9,10]. It is an

*Corresponding author. Tel.: +55 11 3816 9334; fax: +55 11 3816 9325.
E-mail address: mfelinto@ipen.br (M.C.F.C. Felinto).

0022-2313/$ - see front matter © 2007 Elsevier B.V. All rights reserved.
doi:10.1016/j.jlumin.2007.03.016

exothermic reaction between oxidizer (e.g., metal nitrates) and fuel (e.g., urea or glycine). Pechini process is another method very useful for preparing phosphor nanoparticles as powder form using low heating temperature *via* citric acid and ethylene glycol precursors [11–13].

The luminescence efficiency of trivalent rare earth ions (RE^{3+}) doped into inorganic matrices depend on energy transfer from host-to-RE^{3+} ion. It has been shown an increasing of quantum efficiency from (RE^{3+}) doped in nanocrystals with the decreasing of crystals size [14]. Generally, the nanoscale particles are influenced by the presence of a significant number of surface atoms, leading to new optical properties, different from those of bulk samples [15].

$Y_2O_3:Eu^{3+}$ nanoparticles are widely used as red phosphor and display material and have attracted great interest about luminescence properties for the last few years [16–20]. On the other hand, $Y_2O_3:Sm^{3+}$ nanomaterials have been rarely investigated on their photoluminescent properties [21,22].

The Sm^{3+} ion has $4f^5$ configuration and, therefore is labeled as a Kramer ion due to its electronic states that are at least doubly degenerated for any crystal field perturbation [23]. The maximum number of the Stark components for Sm^{3+} ion with $^{2S+1}L_J$ state is $(J+1/2)$-manifold for any symmetry lower than cubic [24]. The spectroscopic investigations of the energy levels of Sm^{3+} ion doped in different hosts have been reported [25,26].

Since samarium compounds have narrow line emission profile and long lifetime as well as europium compounds, it can be used as label in multianalyte assays [27]. Besides, using multiple luminescent labels in the same assay can save time, labor and reagents and also reduces the amount of sample needed [28,29]. It is interesting to use these compounds in a nanometric size once nanoparticles of lanthanide oxides have large Stokes shifts, narrow line-shaped emission bands, long-lived luminescence (approximately 1–2 ms) and also have inherent photostability [30].

The aim of this work is to study the photoluminescence behavior of $Y_2O_3:Sm^{3+}$ nanoparticles prepared *via* combustion and Pechini methods. Nanophosphor system was investigated by using scanning electron microscopy, X-ray diffraction, infrared spectroscopy and luminescent spectroscopy. The intraconfigurational of $^4G_{5/2} \rightarrow {}^6H_J$ transitions ($J = \frac{5}{2}, \frac{7}{2}, \frac{9}{2}$ and $\frac{11}{2}$) of Sm^{3+} ion provide information about its chemical environment and depend on the preparation method and the particle size.

2. Experimental

The starting materials for the synthesis of $Y_2O_3:Sm^{3+}$ system were yttrium and samarium nitrates (synthesized from RE_2O_3–99.9%, Aldrich), glycine (analytical grade, Merck), citric acid (analytical grade, Merck) and ethylene glycol (analytical grade, Merck).

Aqueous stock solution of Y^{3+} and Sm^{3+} nitrates, 1 mol% Sm^{3+} with respect to Y^{3+} were mixed (precursor solution). In the combustion method, stoichiometric glycine-to-nitrate ratio ($G/N = 1.7$) was added in the precursor solution and evaporated on a heater plate. When the excess of water was eliminated, spontaneous ignition occurred at around 300 °C producing a fluffy powder. A thermal treatment was performed at 400, 500 and 600 °C during 1, 5 and 10 h. For Pechini method, citric acid and ethylene glycol compounds were added to precursor solution and heated, under stirring at 90 °C until forming a transparent resin. Leading this resin to 300 °C in a muffle during 2 h, a black solid mass, which was grounded into a powder, was acquired. Finally, this sample was heated at 600 °C for 1, 5 and 10 h.

Infrared absorption spectra (IR) were recorded using Bomen MB 100 spectrometer with KBr pellets, in spectral range from 4000 to 350 cm^{-1}.

X-ray diffraction (XRD) patterns of the samples were conducted with a Rigaku Miniflex using FeKα radiation (30 kV and 15 mA) in an interval of $3-90^\circ$ (2θ) and 1 s of pass time, using the powder XRD method.

Scanning electronic microscopy (SEM) micrographies were obtained in a microscope Philips XR-30 using a sputtering technique with gold as covering contrast material.

The excitation and emission spectra of Y_2O_3 doped compounds were recorded at room and liquid nitrogen temperatures collected at an angle of 22.5° (front face) in a spectrofluorimeter (SPEX-Fluorolog 2) with double grating 0.22 m monochromator (SPEX 1680) using a 450 W xenon lamp as excitation source. Luminescence decay curves were recorded at 298 K using the phosphorimeter (SPEX 1934D) accessory coupled with the spectrofluorimeter.

3. Results and discussion

3.1. *Characterization of* $Y_2O_3:Sm^{3+}$ *samples*

Fig. 1 shows the XRD patterns of synthesized $Y_2O_3:Sm^{3+}$ phosphors with characteristic peaks of standard compound with a cubic structure according to the JCPDS card #25-1200. It was observed that there are no differences in diffraction pattern profiles of the samples treated at 1, 5 and 10 h. For that reason, only XRD patterns of samples prepared with 5 h at different temperatures are shown in Fig. 1. Diffraction lines of nanocrystalline material prepared by Pechini method are broader than lines of powders obtained *via* combustion method, indicating lower crystallite size for the Pechini method. The calculated values of crystallite average sizes were obtained by Scherrer formula. $Y_2O_3:Sm^{3+}$ compound prepared by Pechini (600 °C) and combustion methods (as-prepared, 400, 500 and 600 °C) for 1 h showed an increasing of the crystallite sizes in relation to the temperature (Table 1). In the preparation of $Y_2O_3:Sm^{3+}$ samples by combustion method, the glycine-to-nitrate molar ratio ($G/N = 1.7$) was used. According to Ye et al.

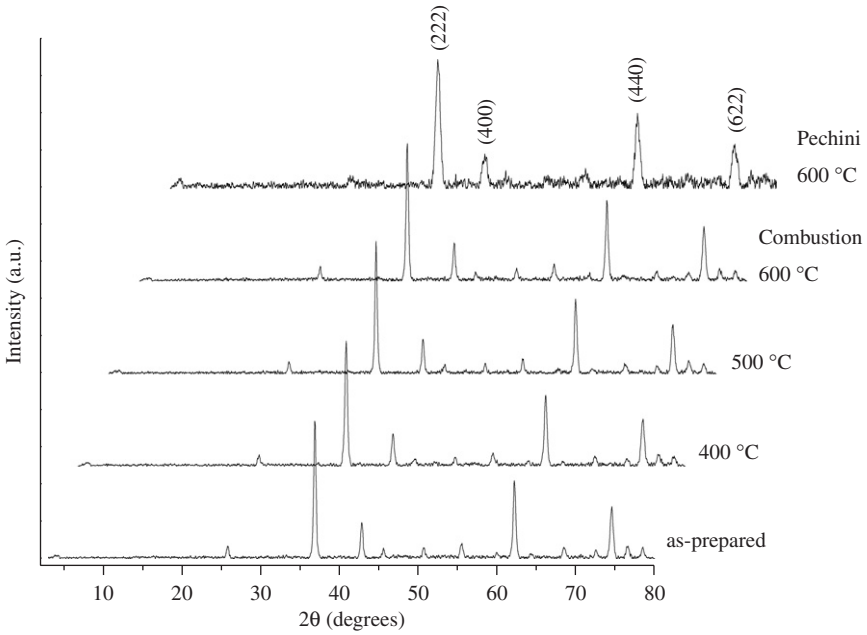

Fig. 1. XRD patterns of $Y_2O_3:Sm^{3+}$ powders obtained by combustion (as-prepared, 400, 500 and 600 °C) and Pechini (600 °C) methods for 5 h.

Table 1
Average particle sizes (nm) of the $Y_2O_3:Sm^{3+}$ compound prepared by Pechini and combustion methods for 1 h

Pechini		Combustion		
600 °C	As-prepared	400 °C	500 °C	600 °C
11.6	26.3	29.8	35.8	38.0

[9], the synthesized $Y_2O_3:Eu^{3+}$ showed that the particle size of the material depends on the flame temperature during reaction, which in turn depends on molar ratio ($G/N = 1.7$ generating 1450 ± 20 °C).

IR spectra of $Y_2O_3:Sm^{3+}$ samples are shown in Fig. 2. Broad bands due to stretching frequency of Y–O can be seen below 700 cm^{-1}. It was observed that Y–O absorption bands broad as particle sizes decrease, probably because the polarization charge induced on the particle surface by external electromagnetic field. It is assumed that when particle sizes decrease, surface effects will be enhanced so that damping of surface mode absorption will increase and Y–O absorption bands become broadened [9]. The low intensity bands in the region from 1200 to 1700 cm^{-1}, were assigned to carbonate species [4] formed by coordination of CO_2 molecules (probably arisen from air absorption) onto Y_2O_3 surface. According to Mokkelbost et al. [31], small amounts of carbonate species are left behind even after calcinations at 1000 °C for 12 h. In addition, bands from spectral range of $3000-3800\,cm^{-1}$ can be attributed to O–H stretching of physiosorbed H_2O or from surface Y–OH groups.

SEM images of $Y_2O_3:Sm^{3+}$ samples (Fig. 3) treated at 600 °C for 5 h showed different agglomerated particles in both Pechini and combustion methods composed of very little particles. The micrographies show different agglomerate shapes such as sponge-like with very slender thickness in three-dimensional network and tablet shape crystallites obtained by combustion and Pechini methods, respectively.

3.2. Luminescence investigation

Fig. 4 exhibits the excitation spectra of $Y_2O_3:Sm^{3+}$ samples prepared ($\lambda_{em} = 608$ nm) by combustion and Pechini processes heated at 400, 500 and 600 °C for 5 h, considering no differences in their optical properties when the samples were also treated at 1 and 10 h. In the range of 250–325 nm, a broad low intensity band placed at around 315 nm is assigned to Y_2O_3 compound used as host material (emission and excitation Y_2O_3 spectra are presented in Fig. 5). This broad band is overlaid by narrow transitions arising from $^6H_{5/2}$ ground state within $4f^5$ configuration of Sm^{3+} ion as prominent peak at 406 nm assigned to the $^6H_{5/2} \rightarrow {}^4K_{11/2}$ transition [32].

These broad bands are related to Y_2O_3 matrix, where excitation band shows maximum value at 315 nm and an emission peak at 360 nm. This broad band is overlaid to narrow lines of intraconfigurational 4f transitions from Sm^{3+} ion and can be observed mainly in $Y_2O_3:Sm^{3+}$ samples prepared by combustion process at lower temperatures.

The Sm^{3+} samples show predominant red emission from $^4G_{5/2} \rightarrow {}^6H_{7/2}$ transition when excited by UV radiation. Photoluminescent behavior presents similar spectral profiles of emission spectra indicating that the Sm^{3+} ion is founded in just one site of symmetry when prepared by combustion and Pechini processes, which is corroborated by luminescence decay data.

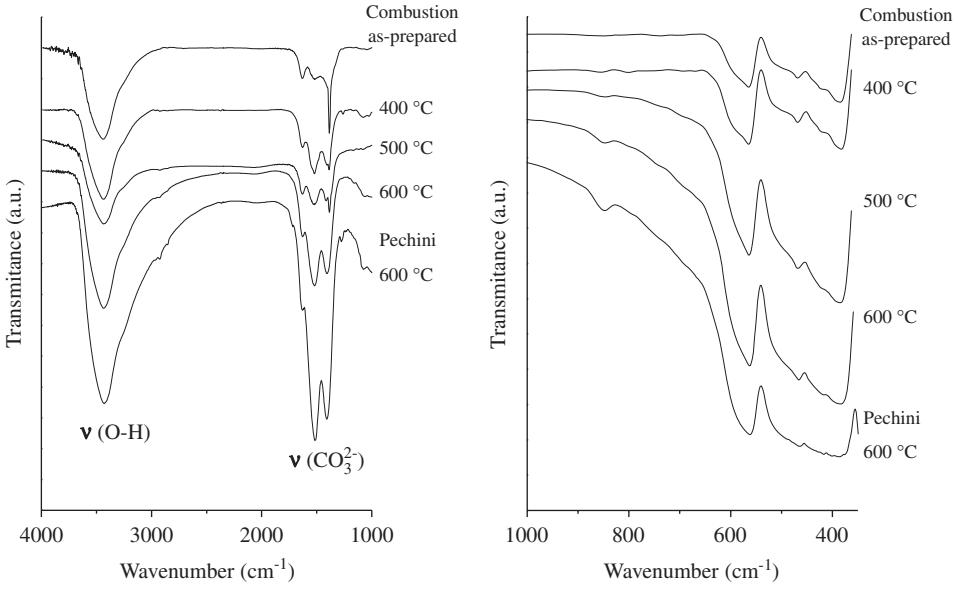

Fig. 2. IR spectra of Y_2O_3:Sm^{3+} samples obtained by combustion (as-prepared, 400, 500 and 600 °C) and Pechini (600 °C) methods for 5 h.

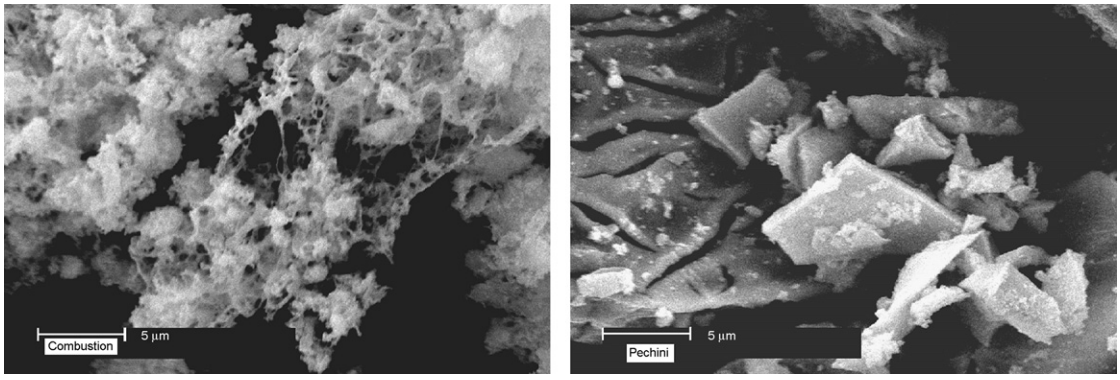

Fig. 3. SEM micrographies of Y_2O_3:Sm^{3+} compounds prepared by combustion and Pechini methods at 600 °C during 5 h.

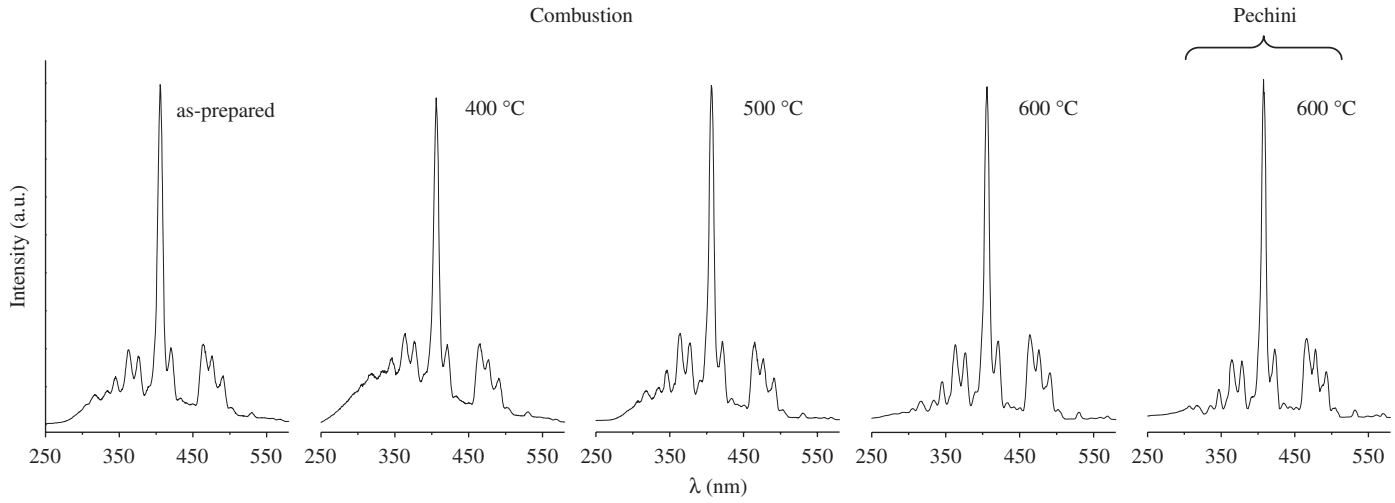

Fig. 4. Excitation spectra of Y_2O_3:Sm^{3+} samples under emission at 608 nm (77 K) prepared by combustion (as-prepared, 400, 500 and 600 °C) and Pechini (600 °C) methods for 5 h.

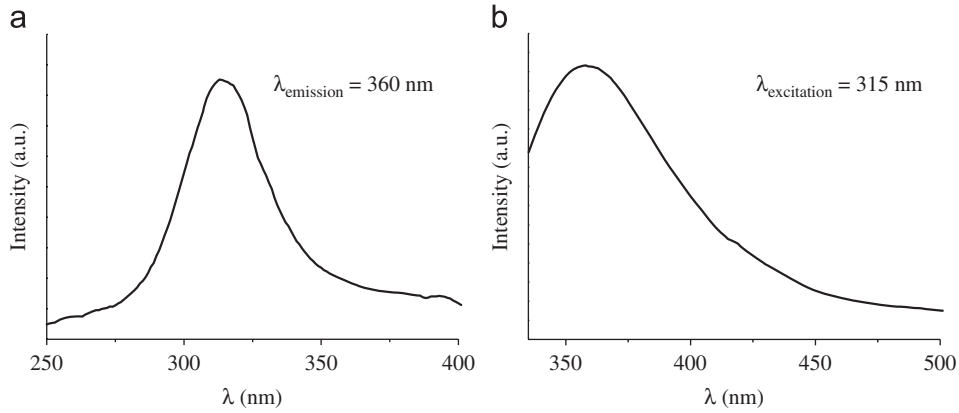

Fig. 5. Photoluminescence spectra of Y_2O_3 matrix recorded at room temperature: (a) excitation and (b) emission.

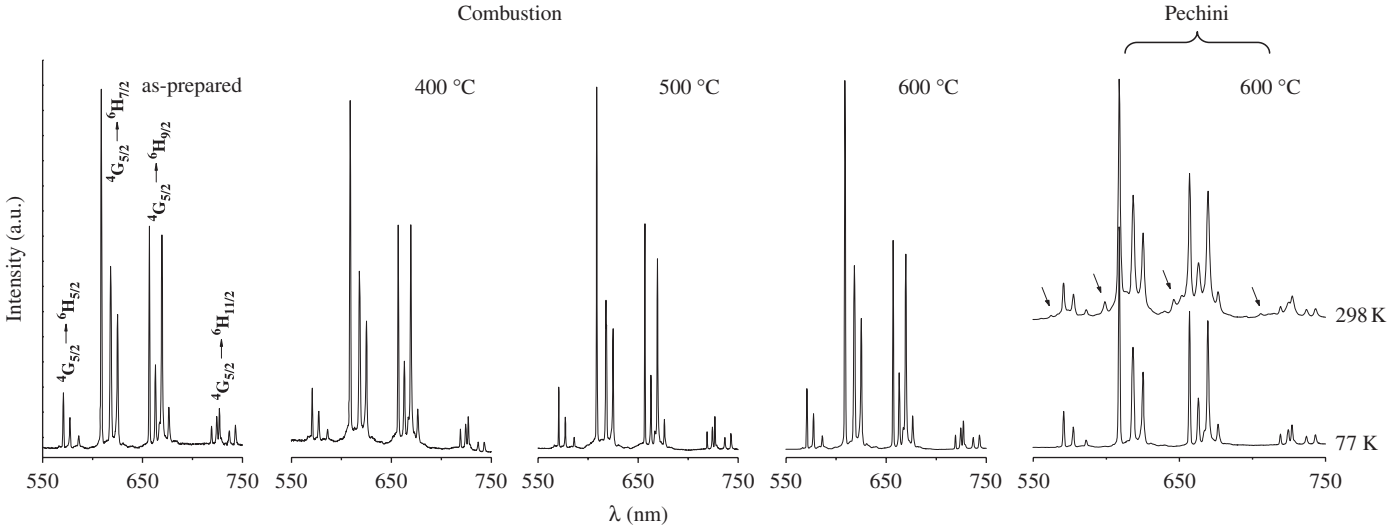

Fig. 6. Emission spectra of Y_2O_3:Sm^{3+} compounds with excitation monitored at 406 nm at 77 K prepared by combustion (as-prepared, 400, 500 and 600 °C) and Pechini (600 °C) methods for 5 h. Lines marked by arrows are bands originating from the upper crystal-field energy levels of excited state $^4G_{5/2}$.

The emission spectra of Y_2O_3:Sm^{3+} samples prepared by combustion and Pechini processes heated at different temperatures (400, 500 and 600 °C) are shown in Fig. 6. The emission narrow peaks of Sm^{3+} ion were attributed as $^4G_{5/2} \rightarrow {}^6H_{5/2}$ (570 nm), $^4G_{5/2} \rightarrow {}^6H_{7/2}$ (610 nm), $^4G_{5/2} \rightarrow {}^6H_{9/2}$ (660 nm) and $^4G_{5/2} \rightarrow {}^6H_{11/2}$ (730 nm) [21,22]. The emission spectra of Y_2O_3:Sm^{3+} systems present similar profiles for combustion and Pechini techniques at several temperatures, with more prominent red emission from $^4G_{5/2} \rightarrow {}^6H_{7/2}$ transition than hypersensitive $^4G_{5/2} \rightarrow {}^6H_{9/2}$transition. Table 2 presents the energy levels of $^4G_{5/2} \rightarrow {}^6H_J$ transitions ($J = \frac{5}{2}$, $\frac{7}{2}$, $\frac{9}{2}$ and $\frac{11}{2}$) observed in the emission spectra of the Y_2O_3:Sm^{3+} based on Fig. 6, in an interval of $570.6 \pm 1.8 \times 10^{-4}$ to $743.2 \pm 1.3 \times 10^{-4}$ nm. Moreover, it is observed that the intraconfigurational transitions of Sm^{3+} ion split in a maximum number of $(J + 1/2)$-manifolds are 3, 4, 5 and 6 energy levels, indicating that Sm^{3+} ion occupies a local site with C_2 symmetry [33,34]. In the emission spectra of samarium samples there are no emission lines shorter than 550 nm (figure not shown).

Photoluminescent behavior shows that Y^{3+} can be replaced by Sm^{3+} species in the Y_2O_3 crystalline lattice once the ionic radii ($Sm^{3+} = 0.104$ nm, $Y^{3+} = 0.093$ nm) [35] as well as the precursor composition are favorable to the formation of the emission centers.

The emission spectra of Y_2O_3:Sm^{3+} samples recorded at room temperature showed low intensity sidebands accompanying the stronger crystal field lines always observed at higher energies [36]. Fig. 6 illustrates the behavior of the compound prepared by Pechini technique at 600 °C for 5 h, registered at 77 and 298 K. Lines marked by arrows are band transitions originated by the upper crystal field energy levels of excited state $^4G_{5/2}$, which may be more populated at 298 K than at 77 K, once in the vibrational spectra these lines are not present. However, these

Table 2
Energy Transitions of the $^4G_{5/2} \rightarrow {}^6H_J$ manifolds (in cm^{-1}) observed in the emission spectra of the $Y_2O_3:Sm^{3+}$ compound prepared by Pechini and combustion methods heated at different temperatures for 5 h

$^4G_{5/2} \rightarrow {}^6H_J$ transitions	As-prepared	Combustion			Pechini
		400 °C	500 °C	600 °C	600 °C
$^4G_{5/2} \rightarrow {}^6H_{5/2}$	17 518	17 520	17 524	17 520	17 515
	17 319	17 319	17 323	17 315	17 319
	17 060	17 061	17 063	17 058	17 060
$^4G_{5/2} \rightarrow {}^6H_{7/2}$	16 427	16 425	16 429	16 421	16 421
	16 180	16 180	16 187	16 200	16 401
	16 035	16 029	16 169	16 173	16 176
	15 999	15 997	15 999	15 994	15 996
$^4G_{5/2} \rightarrow {}^6H_{9/2}$	15 222	15 225	15 225	15 221	15 222
	15 085	15 082	15 086	15 081	15 082
	14 990	14 992	14 997	14 988	14 990
	14 938	14 938	14 938	14 935	14 936
	14 783	14 783	14 787	14 783	14 782
$^4G_{5/2} \rightarrow {}^6H_{11/2}$	13 906	13 903	13 906	13 905	13 905
	13 805	13 804	13 804	13 805	13 802
	13 753	13 755	13 757	13 755	13 753
	13 719	13 723	13 725	13 723	13 721
	13 571	13 569	13 573	13 571	13 568
	13 459	13 460	13 461	13 456	13 459

sidebands are not observed in their emission spectra recorded at liquid nitrogen temperature.

Luminescence decay curves of $^4G_{5/2}$ emitter level of Sm^{3+} doped in Y_2O_3 matrix were recorded monitoring the hypersensitive $^4G_{5/2} \rightarrow {}^6H_{7/2}$ transition at 608.8 nm measured following the 406.0 nm excitation (figure not shown) presenting lifetime values around 1.0 ms at 298 K for samples prepared by both techniques, while Vetrone et al. [22] observed lifetime of 1.6 ms for 1% $Y_2O_3:Sm^{3+}$ compound prepared by combustion method. The mono-exponential behavior observed from the luminescence decay curves of samarium samples confirm the single chemical environment site of Sm^{3+} ion agreeing with $(J + 1/2)$-manifold for the $^4G_{5/2} \rightarrow {}^6H_J$ transition ($J = \frac{5}{2}$, $\frac{7}{2}$, $\frac{9}{2}$ and $\frac{11}{2}$).

4. Conclusion

The $Y_2O_3:Sm^{3+}$ phosphor was prepared by combustion and Pechini methods and thermally treated at different temperatures. XRD patterns showed that the compound is C-form with a cubic structure. IR spectra showed that Y–O absorption bands broad as particle size decreases, probably because the polarization charge induced on the particle surface by external electromagnetic field. The Sm^{3+} samples show predominant red emission from $^4G_{5/2} \rightarrow {}^6H_{7/2}$ transition when excited by UV radiation. Photoluminescent behavior presents similar spectral profiles of emission spectra indicating that the Sm^{3+} ion is found in just one site of symmetry when prepared by combustion and Pechini processes, which is corroborated by luminescence decay data. The crystal field splitting of Sm^{3+} ion has a maximum number of $(J + 1/2)$-manifolds indicating that this ion occupies a C_2 symmetry.

Acknowledgments

The authors thank Fundação de Amparo à Pesquisa do Estado de São Paulo (FAPESP), Conselho Nacional de Desenvolvimento Científico e Tecnológico (CNPq), Rede de Nanotecnologia Molecular e de Interfaces (RENAMI) and Instituto do Milênio de Materiais Complexos (IM^2C) projects for financial support.

References

[1] C. Louis, R. Bazzi, C.A. Marquette, J-L. Bridot, S. Roux, G. Ledoux, B. Mercier, L. Blum, P. Perriat, O. Tillement, Chem. Mater. 17 (2005) 1673.
[2] C.S. Thaxton, N.L. Rosi, C.A. Mirkin, MRS Bull. 30 (2005) 376.
[3] S. Schultz, J. Mock, D.R. Smith, D.A. Schultz, J. Clin. Ligand Assay 22 (1999) 214.
[4] M.R. Davolos, S. Feliciano, A.M. Pires, R.F.C. Marques, M. Jafelicci Jr., J. Solid State Chem. 171 (2003) 268.
[5] S. Ekambaram, J. Alloys Compds. 390 (2005) L1.
[6] G. Concas, G. Spano, E. Zych, J. Trojan-Piegza, J. Phys.: Condens. Matter. 17 (2005) 2597.
[7] J. Bang, M. Abboudi, B. Abrams, P.H. Holloway, J. Lumin. 106 (2004) 177.
[8] M. Kottaisamy, D. Jeyakumar, R. Jagannathan, M.M. Rao, Mater. Res. Bull. 31 (1996) 1013.

[9] T. Ye, Z. Guiwen, Z. Weiping, X. Shangda, Mater. Res. Bull. 32 (1997) 501.
[10] S. Ekambaram, K.C. Patil, M. Maaza, J. Alloys Compds. 393 (2005) 81.
[11] M.U. Pechini, US Patent No. 3330697, 1967.
[12] C.A. Kodaira, H.F. Brito, O.L. Malta, O.A. Serra, J. Lumin. 101 (2003) 11.
[13] C.A. Kodaira, H.F. Brito, M.C.F.C. Felinto, J. Solid State Chem. 171 (2003) 401.
[14] R. Bazzi, M.A. Flores-Gonzalez, C. Louis, K. Lebbou, C. Dujardin, A. Brenier, W. Zhang, O. Tillement, E. Bernstein, P. Perriat, J. Lumin. 102 (2003) 445.
[15] Z. Wei-Wei, X. Mei, Z. Wei-Ping, Y. Min, Q. Ze-Ming, X. Shang-Da, C. Garapon, Chem. Phys. Lett. 376 (2003) 318.
[16] J-W. Wang, Y-M. Chang, H-C. Chang, S-H. Lin, L-C.L. Huang, X-L. Kong, M.W. Kang, Chem. Phys. Lett. 405 (2005) 314.
[17] P.A. Tanner, K.L. Wong, J. Phys. Chem. B 108 (2004) 136.
[18] S. Ray, P. Pramanik, A. Singha, A. Roy, J. Appl. Phys. 97 (2005) art.no. 094312.
[19] N. Vu, T.K. Anh, G-C. Yi, W. Strek, J. Lumin. 122 (2007) 776.
[20] T.L. Phan, M.H. Phan, N. Vu, T.K. Anh, S.C. Yu, Phys. Status Solidi A 201 (2004) 2170.
[21] J.F. Martel, S. Jandl, B. Viana, D. Vivien, J. Phys. Chem. Solids 61 (2000) 1455.
[22] F. Vetrone, J-C. Boyer, J.A. Capobianco, A. Speghini, M. Bettinelli, Nanotechnology 15 (2004) 75.
[23] P.S. May, D.H. Metcalf, F.S. Richardson, R.C. Carter, C.E. Miller, J. Lumin. 51 (1992) 249.
[24] L. Beaury, J. Hölsä, J. Korventausta, J.C. Krupa, R.J. Lamminmäki, P. Porcher, H. Rahiala, E. Säilynoja, Acta Phys. Pol. A 90 (1997) 1203.
[25] J.B. Gruber, Z. Bahram, M.F. Reid, Phys. Rev. 60 (1999) 15643.
[26] S.B. Stevens, C.A. Morrison, M.D. Seltezer, M.E. Hills, J.B. Gruber, J. Appl. Phys. 70 (1991) 948.
[27] P. Huhtinen, M. Kivelä, O. Kuronen, V. Hagren, H. Takalo, H. Tenhu, T. Lövgren, H. Härmä, Anal. Chem. 77 (2005) 2643.
[28] Y-Y. Xu, K. Pettersson, K. Blomberg, I. Hemmillä, H. Mikola, T. Lovgren, Clin. Chem. 38 (1992) 2038.
[29] K. Matsumoto, J. Yuan, G. Wang, H. Kimura, Anal. Biochem. 276 (1999) 81.
[30] M. Nichkova, D. Dosev, R. Perron, S.J. Gee, B.D. Hammock, I.M. Kennedy, Anal. Bioanal. Chem. 384 (2006) 631.
[31] T. Mokkelbost, I. Kaus, T. Grande, M-A. Einarsrud, Chem. Mater. 16 (2004) 5489.
[32] Y. Zhou, J. Lin, S. Wang, J. Solid State Chem. 171 (2003) 391.
[33] H.F. Brito, O.L. Malta, M.C.F.C. Felinto, E.E.S. Teotônio, J.F.S. Menezes, C.F.B. Silva, C.S. Tomiyama, C.A.A. Carvalho, J. Alloys Compds. 344 (2002) 293.
[34] C.A. Kodaira, H.F. Brito, E.E.S. Teotonio, M.C.F.C. Felinto, O.L. Malta, G.E.S. Brito, J. Braz. Chem. Soc. 15 (2004) 890.
[35] J-P.R. Wells, A. Sugiyama, T.P.J. Han, H.G. Gallagher, J. Lumin. 87 (2000) 1029.
[36] X.Y. Chen, M.P. Jensen, G.K. Liu, J. Phys. Chem. B 109 (2005) 13991.